Behavioral/Systems/Cognitive

# Impaired Efficiency of Functional Networks Underlying Episodic Memory-for-Context in Schizophrenia

**Liang Wang,[1,2] Paul D. Metzak,[1,2] William G. Honer,[1,2] and Todd S. Woodward[1,2]**

[1]Department of Psychiatry, University of British Columbia, Vancouver, British Columbia V6T 2A1, Canada, and [2]BC Mental Health and Addictions Research Institute, Vancouver, British Columbia V5Z 4H4, Canada

**Memory for context and episodic memory have been identified as primary contributors to cognitive impairments in schizophrenia. This study examined neural networks involved in episodic memory-for-context in schizophrenia using a multimodal strategy including a graph theoretical approach, combined with an assessment of the contribution of structural impairments to disruption in the efficiency of functional brain networks. Twenty-three patients with schizophrenia and 33 healthy controls performed an episodic memory-for-context task while undergoing functional magnetic resonance imaging scanning. Graph theory was used to characterize the small-world properties of functional connections between activated regions, and a morphometric analysis was used to investigate schizophrenia-related structural deficits. Similar functional activations were identified in the two groups; however, although small-world properties were present in the topological organization of the functional networks in both groups, significant reductions in local, but not global, efficiency were observed in the schizophrenia group. Several key network "hub" regions related to recollection, such as the bilateral dorsal anterior cingulate gyrus, showed reduced gray matter volume in schizophrenia patients. These findings suggest that loss of gray matter volume may contribute to local inefficiencies in the architecture of the network underlying memory-for-context in schizophrenia.**

## Introduction

It is now widely accepted that schizophrenia is characterized by deficits in several domains of cognitive function including attention, memory, and problem solving, with verbal episodic memory being associated with the largest effect size (Heinrichs and Zakzanis, 1998). Neuroimaging investigations of the biological underpinnings of these impaired aspects of cognition have traditionally focused on regions of activation, but new methods of network analysis (for review, see Bullmore and Sporns, 2009) suggest that the optimization of neural networks can be quantitatively measured using graph theoretical approaches. It has been shown that the most efficient systems optimize a balance between local and global connections, referred to as a small-world architecture (Watts and Strogatz, 1998). Small-world properties have been observed in a wide range of environmental, biological, engineering, and socioeconomic systems (Strogatz, 2001), and numerous studies have revealed disease-related abnormalities in small-world properties in functional brain networks (for review, see Bassett and Bullmore, 2009; He et al., 2009a), including in schizophrenia (Micheloyannis et al., 2006; Liu et al., 2008; Bassett et al., 2009; Rubinov et al., 2009). In the current investigation, we apply the small-world approach to the analysis of functional magnetic resonance imaging (fMRI) data collected while performing a verbal episodic memory-for-context task.

Interpreting reality often involves remembering contextual information about an episode; therefore, understanding this aspect of memory (dys)function in schizophrenia is particularly important. For example, when remembering that one's presence has been requested at the police station, a firm grounding in reality requires that one know the context in which that memory was formed (e.g., whether that information was heard, imagined, or read). With respect to neuroimaging, studies of context memory in schizophrenia have typically focused on working memory and on individual regions such as the dorsolateral prefrontal cortex (MacDonald et al., 2005; Simons et al., 2006). Similarly, neuroimaging studies of long-term (episodic) memory typically focus on individual regions such as the lateral prefrontal cortex and the medial temporal lobe (MacDonald et al., 2005; Ravizza et al., 2010). These regions are likely to be major contributors to a functionally linked, large-scale brain network involved in episodic memory-for-context (Bressler and Kelso, 2001).

Structural brain anomalies have been identified in schizophrenia (for review, see Honea et al., 2005), and it has been suggested that a close interaction between brain function and structure may be present (Honey et al., 2009). Thus, using only a single imaging modality to investigate the neural networks involved in complex cognitive tasks may be insufficient, particularly when characterizing disease-related brain abnormalities. In the current study, we combined structural and functional measures to offer a more comprehensive evaluation of the episodic memory-for-context deficits in schizophrenia.

Received July 7, 2010; accepted Aug. 9, 2010.

This study was supported by Canadian Institutes for Health Research (CIHR) Grant MMS 87700 to T.S.W. and W.G.H. T.S.W. was supported by career investigator awards from the CIHR and the Michael Smith Foundation for Health Research (MSFHR). P.D.M. was supported by a trainee award from the MSFHR. The postdoctoral fellowship of L.W. was supported by the BC Mental Health and Addictions Research Institute. We thank Ligaya Allmer, Tonya Kragelj, Rachel Richards, Sarah Flann, Shurin Hase, and Tara Cairo for assistance with data collection, task design, and data management.

Correspondence should be addressed to Dr. Todd S. Woodward, Department of Psychiatry, University of British Columbia, Vancouver, BC V5Z 4H4, Canada. E-mail: todd.woodward@ubc.ca.

DOI:10.1523/JNEUROSCI.3514-10.2010

 0270-6474/10/3013171-09$15.00/0

**Table 1. Demographic and clinical data, behavioral performance, and global anatomic parameters**

| | Patients ($n = 23$) | | Controls ($n = 33$) | | |
|---|---|---|---|---|---|
| Variable | *n* | % | *n* | % | $p^a$ |
| Right handed | 23 | 100 | 32 | 97 | 0.86 |
| Male | 15 | 65.2 | 16 | 48.5 | 0.30 |
| | Mean | SD | Mean | SD | $p^b$ |
| Age (years) | 30.0 | 9.2 | 27.3 | 7.6 | 0.24 |
| Quick IQ (Ammons and Ammons, 1962) | 102.5 | 12.1 | 102.4 | 10.2 | 0.98 |
| Socioeconomic status (Hollingshead and Redlich, 1958) | 52.7 | 21 | 57.3 | 22.1 | 0.50 |
| Dosage of antipsychotic medication [chlorpromazine equivalents/d (mg)] (Bezchlibnyk-Butler and Jeffries, 2005) | 122 | 101.8 | | | |
| Age of onset | 21.9 | 5.6 | | | |
| Illness duration (years) | 8.1 | 8.0 | | | |
| SSPI (Liddle et al., 2002) | 12.1 | 5 | | | |
| Episodic memory-for-context task | | | | | |
| Accuracy (%) | 74.2 | 12.7 | 82.7 | 0.1 | 0.005 |
| Reaction time (s) | 1.03 | 0.24 | 0.95 | 0.18 | 0.21 |
| Global anatomic parameters ($mm^3$) | | | | | |
| Gray matter volume | 714.9 | 71.8 | 705.4 | 55.0 | 0.57 |
| White matter volume | 462.5 | 41.8 | 447.0 | 39.0 | 0.16 |
| Total intracranial volume | 1805.3 | 121.9 | 1731.0 | 128.0 | 0.03 |

[a] *p* values are obtained from a two-tailed $\chi^2$ test.

[b] *p* values are obtained from a two-sample *t* test, two-tailed.

The context memory task we investigated involved an initial nonscanned task session, where subjects encountered words in four different task contexts: solving, hearing, associating, and reading. Functional and structural MRI scanning was performed during the subsequent recall run, where participants were asked to indicate the task context in which they had encountered the presented word. We hypothesized that schizophrenia patients would show performance deficits, as well as abnormalities, in functional activation in several regions underlying abnormal context memory in schizophrenia. We also hypothesized that schizophrenia patients would display a reduced coordination of functional brain activity patterns compared with healthy controls and that the altered topological organization of functional networks would be related to structural deficits in several key regions, such as dorsal prefrontal regions.

## Materials and Methods

### *Participants*

Twenty-three patients were recruited from psychiatric hospitals and community health agencies in and around Vancouver, British Columbia, Canada, with diagnoses of schizophrenia ($n = 15$) or schizoaffective disorder ($n = 8$). Diagnosis was based on a multidisciplinary team conference during the first month of admission when all sources of information are reviewed. The Mini-International Neuropsychiatric Interview (Sheehan et al., 1998) was administered on the date of MRI testing to confirm diagnosis. Psychopathology was assessed using the Signs and Symptoms of Psychotic Illness scale (SSPI) (Liddle et al., 2002), a scale gauging symptom severity using 20 symptom items scored between 0 and 4 (Table 1). Patients with schizophrenia did not differ significantly from patients with schizoaffective disorder on age, education, medication level, intelligence quotient (IQ) estimate, symptom severity (as measured by the SSPI total score), accuracy performance, and reaction time. Thus, these patients were pooled and are referred to hereafter as the schizophrenia group. Participants were excluded if they had ever suffered a head injury or a concussion resulting in a loss of consciousness for ≥10 min, if they had ever been diagnosed with a neurological disease or illness, or if they had current and/or past problems with substance abuse (including alcoholism). Substance abuse was assessed by chart review and by interview, and participants were also excluded if they met the DSM IV (*Diagnostic and Statistical Manual of Mental Disorders*, fourth revision) criteria for an Axis I diagnosis of a substance-related disorder (e.g., polysubstance dependence). All patients but one were taking stable doses of antipsychotic medications at the time of testing, with the large majority taking atypical antipsychotics (for dosage information, see Table 1).

Thirty-three healthy controls were recruited through advertisement and word-of-mouth. Screening with a medical questionnaire ensured that none of the healthy participants had any current or prior history of psychiatric illness. Additional exclusion criteria were the same as those used for the patient groups. All participants gave written informed consent after a full explanation of the study and the procedures involved. All experimental procedures were approved by the University of British Columbia Clinical Research Ethics Board.

### *Procedure*

The stimuli consisted of 120 well known words; four sets of 30 words were presented in each of four task contexts: solving, hearing, associating, and reading. The words used in this study were common nouns chosen from the English Lexicon Project (http://elexicon.wustl.edu/) (Balota et al., 2007) to have a standard word length (ranging from 4 to 10 letters; mode, 6 letters) and log-transformed Hyperspace Analog to Language frequency (Lund and Burgess, 1996) ranging from 4 to 11. The word-set/task condition assignments were randomly assigned for each individual subject. On all solving and hearing trials, a jumbled word puzzle was presented on the computer screen in conjunction with a clue about the meaning of the word. For example, jumbled letters such as "BERAZ" may be presented, with a clue such as "a striped grazing animal," the answer being "ZEBRA." Thirty of the word puzzle trials were designated "solving" trials in which subjects were required to solve the puzzle themselves and say the answer aloud before pressing a button to advance to the next trial. The other 30 puzzle trials were "hearing" trials in which a digitized recording of the solution was played when the jumbled word was presented. For the "associating" trials, a correctly spelled reference word was presented with the instruction to indicate which of the two words presented below it was most closely associated with the reference word by pressing one of the two keys. Subjects were required to press the left key if the word on the left was more associated with the reference word and vice versa. For each reference word, a strongly associated word and a weakly associated word were presented, with the relationships selected based on the Edinburgh Associative Thesaurus (Kiss et al., 1973). For the silent "reading" trials, a correctly spelled word was presented with the following instruction: "Please read silently." Subjects were required to press a button after they had finished reading the word silently to advance to the next trial.

The task execution run was self-paced, with the initiation of a new trial commencing 1, 2, or 3 s (randomly determined) after the subject's response. The exception to this rule was the associating condition, in which the to-be-associated words were left on the screen for 3 s and were accompanied by the instructions to "think about the association for the entire time the words are displayed on the screen." All words used were concrete nouns.

Following this nonscanned task session, these words were used as targets during the scanned recall phase. Approximately 10 min after the end of the task run, a 15.5 min recall run was performed while subjects were being scanned. The subjects were informed about the memory component of the task only once being prepared to enter the scanner. The recall run consisted of 120 trials using all the same words presented in the task execution run, divided into six alternating blocks of 20 trials and 140 s each, in which the participant was asked to indicate in which task condition that word had been encountered previously. During each trial, a single word was presented in the center of the screen with a reminder instruction cue at the bottom of the screen. While a word was being displayed, participants were asked to judge whether the word was read or associated, or whether the participant or the computer had solved the puzzle. In all conditions, participants indicated their response by pressing the left or right key on a MRI-compatible response box with their

right hand. For each trial, words were presented for a maximum of 5 s; however, the word disappeared from the screen if a response was made, and the screen remained blank for the remainder of the 5 s period. Each trial was separated by a varying intertrial interval of 1, 2, or 3 s, which included a 1 s fixation crosshair. In addition, to avoid multicolinearity (Cairo et al., 2004), a 10 s blank trial was inserted after each block. The word "relax" was presented for the first 9 s of each blank trial, followed by a 1 s crosshair to cue subjects that a new trial was about to begin. Trials were blocked as opposed to randomly presented to avoid costs and activations associated with switching tasks (Ruff et al., 2001; Rushworth et al., 2002; Woodward et al., 2006a).

### *Image acquisition*

Imaging was performed at the University of British Columbia MRI Research Centre on a Phillips Achieva 3.0 tesla MRI scanner with quasar dual gradients (maximum gradient amplitude, 80 mT/m; maximum slew rate, 200 mT/m/s). The participant's head was firmly secured using a customized head holder. Functional image volumes were collected using a T2*-weighted gradient-echo spin pulse sequence [36 axial slices; thickness/gap, 3/1 mm; matrix, 80 × 80; repetition time (TR), 2000 ms; echo time (TE), 30 ms; flip angle (FA), 90°; field of view (FOV), 240 × 240 mm] effectively covering the whole brain. Each scan lasted for 920 s, and 460 image volumes were obtained. The structural scan comprised a sagittal three-dimensional T1-weighted gradient-echo sequence (T1TFE sequence) over the whole brain: 182 slices; thickness/gap, 1.0/0 mm; matrix, 256 × 256; TR, 8.13 ms; TE, 3.7 ms; FA, 8°; FOV, 182 × 256 mm.

### *Image preprocessing and analysis*

*Functional imaging.* fMRI data were preprocessed using SPM5 (http://www.fil.ion.ucl.ac.uk/spm/). Translation and rotation corrections for head movements did not exceed 3 mm or 3° for each participant. The data were then spatially normalized to an echo-planar imaging (EPI) template in Montreal Neurological Institute (MNI) stereotaxic space using an optimum 12-parameter affine and nonlinear cosine basis function transformation. The normalized volumes were resampled to 3 mm cubic voxels and spatially smoothed with an 8 mm full-width at half-maximum (FWHM) isotropic Gaussian kernel. A high-pass filter of 1/128 Hz was used to remove low-frequency noise, and an AR(1) model corrected for temporal autocorrelation.

The four event types (solving, hearing, associating, and reading) were separately defined for each subject, consisting of four regressors. Events for each of the regressors were modeled as predictor variables by convolving onset times of trials responded correctly (Gur and Gur, 1995) with a canonical hemodynamic response function. The regression coefficient for each regressor was estimated, and contextual recollection involved the contrast between all correct trials and baseline. The contrast images from each subject were entered into the second level of analysis, treating subjects as a random effect, and statistical inference was conducted by using two-sample *t* tests. Age, gender, and the interaction of age and gender were added as covariates in this analysis to eliminate the influence of these confounds on brain activations observed. Statistical parametric maps of the contrast were then constructed where significantly activated regions consisted of eight or more contiguous voxels at an $\alpha$ threshold of 0.05 corrected for family-wise error (FWE) within the whole brain. Since there were no significant statistical differences between healthy controls and patients with schizophrenia (see Results), we focused on the regions of activation common to both groups for subsequent analyses. To investigate whether patients with schizophrenia display abnormal topological organization in task-related functional networks, we defined regions of interest (ROIs) as nodes in the networks by parcellating the common activation map into separate ROIs using the Automated Anatomical Labeling template (Tzourio-Mazoyer et al., 2002).

*Structural imaging.* Structural data (see supplemental material, available at www.jneurosci.org, for scanning parameters) were analyzed using the VBM5 (Voxel-Based Morphometry 5) toolbox (http://dbm.neuro.uni-jena.de). To analyze volume differences between the two groups, the gray matter tissue maps were modulated by the Jacobian determinants of the deformation parameters obtained via normalization to the MNI standard space. Gray matter volume was then smoothed using an 8 mm FWHM Gaussian kernel and used for a second-level statistical analysis using a two-sample *t* test in SPM5. Age, gender, the interaction of age and gender, and total intracranial volume were used as covariates in this analysis. Statistical inference started with the definition of a primary threshold ( $p < 0.001$, uncorrected) to identify contiguous voxels. Then, an FWE-corrected cluster-size $\alpha$ threshold of 0.05 was used that produced a minimum spatially adjusted extent threshold of 1200 1 mm isotropic voxels (Hayasaka et al., 2004).

### *Functional connectivity*

Second-level parameters were used to assess connectivity (Rissman et al., 2004; Woodward et al., 2006b). For each of the ROIs, contrast image values (control group, 33 images; patient group, 23 images) within each group were obtained by averaging the contrast values over all the voxels within each region. Functional connectivity examines interregional correlations in neuronal activity (Friston et al., 1993). Partial correlation can be used as a measure of the functional connectivity between a given pair of regions by attenuating the contribution of other sources. In this study, we used partial correlations to reduce indirect dependencies on other brain areas and build undirected binary graphs. The partial correlation coefficient between amplitude series within each group in regions *i* and *j* was measured as follows:

$$r_{i,j} = -S_{i,j}^{-1} / \sqrt{S_{i,i}^{-1} \times S_{j,j}^{-1}},$$

where $s_{i,j}$ represents a sample covariance value between the contrast values from the two regions across the subjects, and $S_{i,j}^{-1}$ denotes the $(i, j)$th array of the inverted covariance matrix calculated from all possible pair of regions.

### *Graph theoretical analysis*

*Construction of functional brain networks.* The functional connectivity matrix was first converted to a binary graph (i.e., network). To avoid the influence of strength of interregional correlations between groups, network sparsity (i.e., the ratio between the number of existing edges and all the possible edges) was used as a threshold applied to build the graph (Achard and Bullmore, 2007; Wang et al., 2009). As there is currently no formal consensus regarding threshold selection, we investigated the properties of the networks over a wide range of values from 0.12 to 0.33 using increments of 0.01. The lower bound of the threshold interval allowed the small-world properties to be properly estimated and networks to be connected, whereas the upper bound was used to ensure that the global efficiency of the real networks was less than that of random networks (Achard and Bullmore, 2007). Thus, the threshold range corresponds to a small-world regime.

*Measures of functional brain networks.* The application of graph theoretical approaches to a binary graph allowed the characterization of the small-world properties. Small-world properties of a network are traditionally characterized by the clustering coefficient ($C_p$) and the shortest path length ($L_p$) of the network (Watts and Strogatz, 1998). As graph theoretical approaches have developed, alternative metrics based on network efficiency (Latora and Marchiori, 2001) have received growing attention. Several applications of this novel approach have suggested that functional brain networks do possess efficient small-world properties at a low cost (Achard and Bullmore, 2007; Wang et al., 2009).

Briefly, the efficiency of a graph (or network) *G* is defined as the inverse of the harmonic mean of the shortest path length $l_{i,j}$ from node *i* to node *j*:

$$E(G) = \frac{1}{N_G(N_G - 1)} \sum_{i \neq j \in G} \frac{1}{l_{ij}}.$$

When *G* represents a whole network, this metric measures the efficiency over the whole graph, known as global efficiency $E_{\text{glob}}$; $N_G$ denotes the number of nodes in the whole network. In contrast, when *G* is a subgraph as the set of nodes that are immediate neighbors of a node *i* (i.e., directly connected to a node with an edge), this index measures the efficiency over the subgraph, known as local efficiency of the node *i*, where $N_G$ denotes the number of nodes in the subgraph. Thus, local efficiency $E_{\text{loc}}$

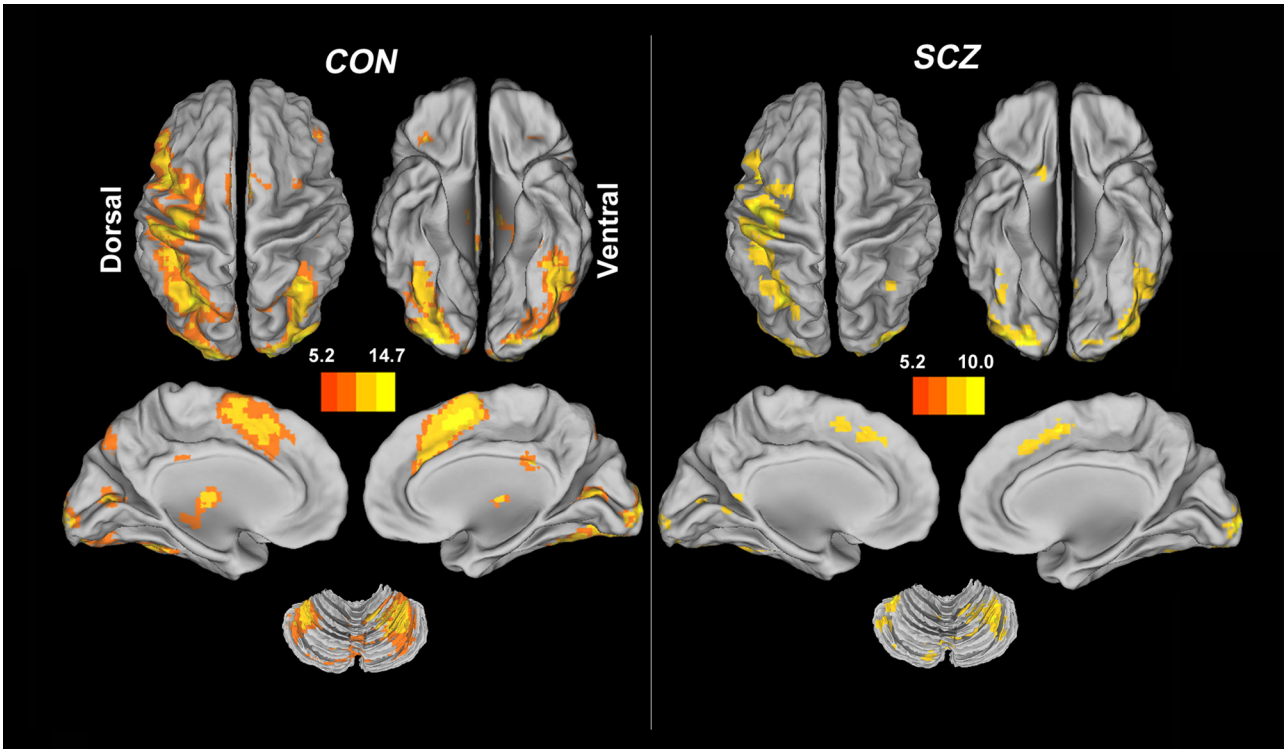


**Figure 1.** Functional activations. Functional activation maps correspond to the contrast between correct contextual recollection and baseline in healthy controls (CON) and patients with schizophrenia (SCZ). No significant differences in activations were found between the two groups ( $p < 0.05$, corrected for FWE). The pictures and following brain maps are shown on the surface of the brain using the CARET software (http://brainvis.wustl.edu/wiki/index.php/Caret:About). See Table 2 for the peak coordinates for each group and both groups together; see supplemental Figure S1 for a map of the regions common to both groups and supplemental Table S2 for a list for these regions (available at www.jneurosci.org as supplemental material).

of the whole graph is defined as the average of local efficiency over the subgraphs.

Finally, nonparametic permutation tests were applied to determine the statistical significance of the differences in network parameters ($E_{glob}$ and $E_{loc}$) between the two groups. First, the two metrics were computed separately for each group over the range of sparsity thresholds. To test the null hypothesis that the observed group difference in each metric could occur by chance, we randomly reallocated each subject to one of the two groups and recomputed functional connectivity matrix based on the new amplitude series from each randomized group. The same network metrics ($E_{glob}$ and $E_{loc}$) were repeatedly calculated 1000 times, and a randomized null distribution based on between-group differences in each metric was created at each threshold. Then the 95% percentile point of the distribution was used as the critical value for a one-tailed test of the null hypothesis.

## Results

### Demographic data and behavioral results

Demographic and clinical data for the schizophrenia patients and healthy controls are shown in Table 1. No significant differences between both groups were observed in age, gender, IQ, and socioeconomic status. Behavioral performance between groups was analyzed by way of a repeated-measures ANOVA with context (solving, hearing, associating, and reading) as a within-subject factor and group (patients vs controls) as a between-subject factor. With respect to accuracy, a significant group effect was observed ($F_{(1,54)} = 8.63$; $p = 0.005$) with no significant context effect ($F_{(3,162)} = 0.44$; $p = 0.72$) or interaction ($F_{(3,162)} = 2.134$; $p = 0.1$). With respect to reaction time (correct trials only), the group effect ($F_{(1,54)} = 1.80$; $p = 0.19$) and interaction ($F_{(1,54)} = 0.26$; $p = 0.85$) were not significant. However, a significant context effect was observed ($F_{(3,162)} = 32.91$; $p < 0.001$), whereby reaction times were longer in the hearing and reading conditions (mean of 1.02 and 1.14 s, respectively) relative to the solving and associating conditions (mean of 0.87 and 0.94 s, respectively). Two-sample $t$ tests of the overall accuracy and reaction time were conducted between the two groups, and the results are displayed in Table 1.

### Functional activations

Figure 1 suggests that healthy subjects and schizophrenia patients showed a similar pattern of activation while performing the contextual memory task. Regions were deemed as being significantly active if their activity exceeded an $\alpha$ threshold of 0.05 corrected for voxel-wise FWE within the whole brain. For healthy controls, the activated clusters involved the left inferior occipital gyrus extending to the right lingual gyrus, right supplementary motor area extending to the left median cingulate gyrus, left inferior orbitofrontal gyrus, right middle frontal gyrus, right precentral gyrus, bilateral thalamus, left hippocampus, and basal ganglia (Table 2, top). Similarly, patients showed significant activations in the right middle occipital gyrus extending to the right lingual gyrus, left precentral gyrus extending to the left inferior parietal lobule, left inferior occipital gyrus extending to the left cerebellum, left supplementary motor area extending to the left medial superior frontal gyrus, left calcarine fissure, left insula, left thalamus, right angular, and right middle frontal gyrus (Table 2, middle). The group difference was nonsignificant ( $p < 0.05$, corrected for FWE). The clusters representing shared activations (conjunctions) across the two groups include the right middle occipital gyrus, precentral gyrus extending into left inferior parietal lobule, left inferior occipital gyrus extending to the left cerebellum, left supplementary motor area, left insula, and left thalamus (Table 2, bottom; supplemen-

**Table 2. Regions with significant activations associated with contextual memory in each group and common to both groups**

| Group and region | Volume (mm$^3$)[a] | Peak MNI coordinate | | | Z |
|---|---|---|---|---|---|
| | | x | y | z | |
| Controls | | | | | |
| Inferior occipital gyrus | 179,793 | −24 | −99 | −12 | 7.94 |
| Lingual gyrus | — | 24 | −98 | −9 | 7.87 |
| Inferior occipital gyrus | — | −33 | −90 | −9 | 7.84 |
| Supplementary motor area | 22,599 | 3 | 9 | 51 | 7.42 |
| Supplementary motor area | — | 9 | 0 | 60 | 7.70 |
| Dorsal cingulate gyrus | — | −6 | 15 | 39 | 7.07 |
| Thalamus | 5,292 | −12 | −18 | 9 | 7.18 |
| Hippocampus | — | −21 | −27 | −6 | 5.84 |
| Pallidum | 2,241 | −15 | 6 | 3 | 6.52 |
| Thalamus | 783 | 12 | −18 | 9 | 6.33 |
| Inferior frontal gyrus (orbital) | 1,485 | −30 | 27 | −6 | 6.32 |
| Posterior cingulate gyrus | 1,188 | 0 | −33 | 27 | 6.30 |
| Middle frontal gyrus | 1,863 | 54 | 36 | 21 | 6.27 |
| Middle frontal gyrus | — | 45 | 36 | 18 | 5.96 |
| Insula | 3,003 | 33 | 24 | −6 | 6.17 |
| Caudate | 2,079 | 15 | 9 | 9 | 6.15 |
| Pallidum | — | 12 | 6 | −3 | 5.55 |
| Precentral gyrus | 432 | 63 | 3 | 24 | 5.72 |
| Precentral gyrus | 405 | 54 | 6 | 39 | 5.52 |
| Middle frontal gyrus | 405 | 33 | 0 | 57 | 5.31 |
| Supramarginal gyrus | 189 | 45 | −33 | 42 | 5.20 |
| Patients | | | | | |
| Middle occipital gyrus | 1,755 | 27 | −96 | 12 | 7.61 |
| Middle occipital gyrus | — | 36 | −90 | −2 | 6.98 |
| Lingual gyrus | — | 24 | −90 | −12 | 6.83 |
| Precentral gyrus | 38,718 | −42 | 9 | 30 | 7.50 |
| Inferior parietal lobule | — | −45 | −27 | 48 | 7.43 |
| Precentral gyrus | — | −39 | −15 | 57 | 7.41 |
| Inferior occipital lobule | 21,627 | −21 | −99 | −12 | 7.41 |
| Cerebellum VI | — | −39 | −42 | −30 | 6.82 |
| Supplementary motor area | 5,805 | −3 | 6 | 51 | 6.42 |
| Superior frontal gyrus (medial) | — | −3 | 18 | 42 | 6.37 |
| Calcarine fissure | 567 | −6 | −57 | 3 | 5.87 |
| Insula | 540 | −27 | 24 | −3 | 5.60 |
| Cerebellum IX | 702 | −3 | −57 | −39 | 5.54 |
| Calcarine fissure | 594 | −12 | −75 | 3 | 5.36 |
| Thalamus | 189 | −15 | −21 | 6 | 5.29 |
| Angular gyrus | 729 | 33 | −57 | 48 | 5.13 |
| Superior parietal gyrus | — | 36 | −66 | 57 | 5.13 |
| Middle frontal gyrus | 216 | 36 | 0 | 60 | 4.96 |
| Common regions | — | | | | |
| Middle occipital gyrus | 16,956 | 27 | −96 | 12 | 7.61 |
| Middle occipital gyrus | — | 36 | −90 | −2 | 6.98 |
| Lingual gyrus | — | 24 | −90 | −12 | 6.83 |
| Precentral gyrus | 36,639 | −42 | 9 | 30 | 7.50 |
| Inferior parietal lobule | — | −45 | −27 | 48 | 7.43 |
| Precentral gyrus | — | −39 | −15 | 57 | 7.41 |
| Inferior occipital gyrus | 17,253 | −21 | −99 | −12 | 7.41 |
| Cerebellum VI | | −39 | −42 | −30 | 6.82 |
| Supplementary motor area | 5,778 | −3 | 6 | 51 | 6.42 |
| Superior frontal gyrus (medial) | — | −3 | 18 | 42 | 6.37 |
| Cerebellum crus I | 2,835 | −9 | −81 | −24 | 6.20 |
| Vermis VII | — | 3 | −75 | −21 | 5.78 |
| Insula | 540 | −27 | 24 | −3 | 5.60 |
| Cerebellum IX | 702 | −3 | −57 | −39 | 5.54 |
| Calcarine fissure | 540 | −12 | −75 | 3 | 5.36 |
| Thalamus | 189 | −15 | −21 | 6 | 5.29 |
| Angular gyrus | 729 | 33 | −57 | 48 | 5.13 |
| Superior parietal gyrus | — | 36 | −66 | 57 | 5.13 |

[a]Number of contiguous active voxels × 27 mm$^3$ (3 × 3 × 3). Coordinates of activation peaks are assigned to anatomical regions by means of automated anatomical labeling (Tzourio-Mazoyer et al., 2002). If there are multiple peak points in each significant cluster, the first three points are marked by — below the cluster size of each cluster. The same notation is applicable to Table 3.

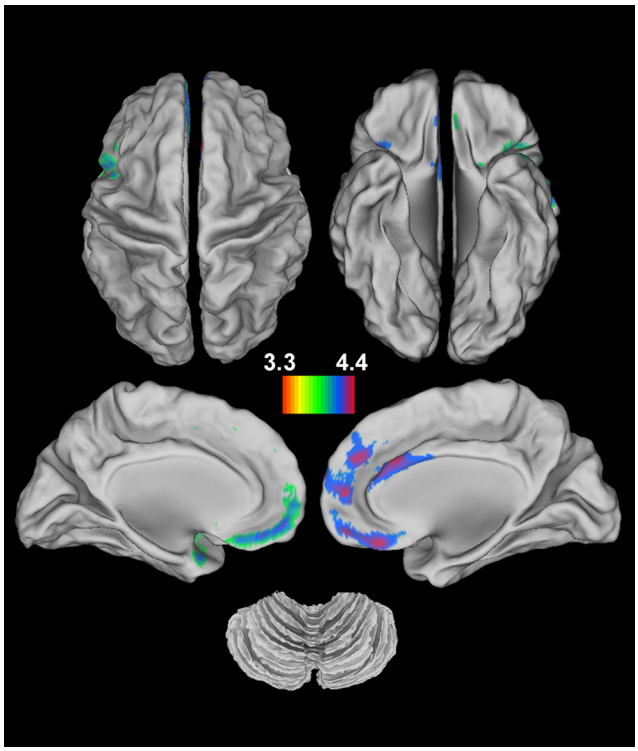


**Figure 2.** Structural deficits in schizophrenia. Significant reductions in gray matter volume are observed in patients with schizophrenia compared with healthy controls ( $p < 0.05$, corrected for FWE). No significant increases are found in schizophrenia. See Table 3 for the peak coordinates of areas with significant structural differences.

tal Fig. S1, red clusters, available at www.jneurosci.org as supplemental material). Within the common domain, there was also no significant activation difference between the two schizophrenia subsets. In total, the common activations were categorized into 43 ROIs (supplemental Table S2, available at www.jneurosci.org as supplemental material).

At a more liberal threshold ( $p < 0.001$, noncorrected), comparison between the two groups showed significantly decreased activations in bilateral prefrontal cortex (supplemental Table S1 supplemental Fig. S1, green clusters, available at www.jneurosci.org as supplemental material), indicating that schizophrenia patients show prefrontal dysfunction when performing a context recollection task. Besides this abnormal prefrontal activity, inferior and middle occipital gyrus, thalamus, and caudate also showed decreased activity in schizophrenia (supplemental Table S1, available at www.jneurosci.org as supplemental material), whereas no significantly increased activity was found in the schizophrenia group. However, the regions found to have decreased activation for schizophrenia when using a lower threshold were essentially nonoverlapping with the ROIs (i.e., those showing common activations between the patients and controls).

### Structural impairments in gray matter volume

Global gray and white matter did not differ between the two groups (Table 1), whereas total intracranial volume was higher in patients than controls. At $p < 0.05$ (FWE cluster-level correction), seven distinct clusters of reductions in gray matter volume were identified in schizophrenia patients compared with the healthy controls (Fig. 2). Structural differences were most pronounced in the insula extending into pars opercularis of the left inferior frontal gyrus, left middle occipital gyrus, right pars trian-

**Table 3. Regions demonstrating significant reductions in gray matter volume in schizophrenia**

| Contrast and region | Volume ($mm^3$)[a] | Peak MNI coordinate | | | Z |
|---|---|---|---|---|---|
| | | x | y | z | |
| Controls > patients | | | | | |
| Insula | 29,500 | −38 | 8 | −11 | 5.20 |
| Insula | — | −38 | 8 | −2 | 5.04 |
| Inferior frontal gyrus (opercular) | — | −48 | 8 | 25 | 4.85 |
| Anterior cingulate gyrus | 12,314 | −31 | −95 | 7 | 4.34 |
| Middle occipital gyrus | 2,736 | 55 | 33 | 15 | 4.29 |
| Middle occipital gyrus | 3,065 | 57 | 23 | 20 | 4.19 |
| Inferior frontal gyrus (triangular) | 1,315 | 52 | 39 | −5 | 4.12 |
| Inferior frontal gyrus (triangular) | — | 37 | 21 | 0 | 3.64 |
| Inferior frontal gyrus (opercular) | — | 39 | 14 | −9 | 3.59 |
| Insula | 1,606 | 43 | 6 | 1 | 4.12 |
| Insula | — | −24 | 8 | 56 | 4.05 |
| Insula | — | −33 | 10 | 57 | 3.81 |
| Middle frontal gyrus | 1,265 | −29 | 0 | 61 | 3.91 |
| Middle frontal gyrus | — | −38 | 8 | −11 | 3.77 |
| Precentral gyrus | — | −38 | 8 | −2 | 3.41 |

[a]Number of contiguous active voxels × 1 $mm^3$ (1 × 1 × 1). See Table 2 footnote.

**Table 4. Regions showing overlap between the functional activations common to both groups and the gray matter volume reductions in schizophrenia**

| Region | Side | Volume ($mm^3$)[a] | Hub (SCZ/CON)[b] |
|---|---|---|---|
| Inferior frontal gyrus (opercular) | L | 621 | No/No |
| Supplementary motor area | L | 297 | No/No |
| Precentral gyrus | L | 297 | Yes/No |
| Inferior frontal gyrus (triangular) | L | 297 | Yes/No |
| Inferior occipital gyrus | L | 189 | Yes/No |
| Superior frontal gyrus (medial) | L | 270 | No/Yes |
| Dorsal anterior cingulate gyrus | L | 378 | No/Yes |
| Dorsal anterior cingulate gyrus | R | 81 | No/Yes |
| Lingual gyrus | L | 135 | No/Yes |
| Middle occipital gyrus | L | 972 | Yes/Yes |

[a]Number of contiguous voxels × 27 $mm^3$ (3 × 3 × 3).

[b]Hub-associated regions in the schizophrenia (SCZ) and/or healthy control (CON) groups.

gularis and opercularis of inferior frontal gyrus, right insula, and left middle frontal gyrus extending to the precentral gyrus (Table 3). No increases were found in the schizophrenia group. In addition, we did not find significant correlations between gray matter volume and accuracy performance at the same threshold above, implying that the structural deficits in schizophrenia were unlikely to be related to relatively poor behavioral performance. Several of the regions with structural differences overlapped with the functional activations elicited by the contextual memory task (Table 4).

### Small-world properties

The application of graph theoretical approaches demonstrated that the functional brain networks of both healthy controls and schizophrenia patients showed small-world properties with high global (Fig. 3*A*) and local (Fig. 3*B*) efficiency. However, significant reductions in local, but not in global, efficiency were observed in schizophrenia patients over a wide range of thresholds ($0.15 < \text{sparsity} < 0.26$ highlighted by the gray area) using nonparametric statistical tests ($p < 0.05$). In addition, we investigated the degree distribution in the functional brain networks and found that the distribution patterns of both groups were similar and met a power law of the form $p(k) \sim K^{-\alpha}$ (supplemental Fig. S2, available at www.jneurosci.org as supplemental material), consistent with previous studies (Eguiluz et al., 2005; van den Heuvel et al., 2008).

### Network hubs

To investigate the cause of the disorder-related network inefficiency, we compared connection degree of each ROI between the two groups over the threshold range ($0.15 < \text{sparsity} < 0.26$). A region is denoted as a hub if the degree of this node is at least 1 SD greater than the average degree over all nodes in the network. To avoid the effect of specific threshold selection on hub categorization, hubs were determined by calculating the cumulative sum of the value of each region at each threshold (equal to 1 if the region is a hub, otherwise to zero) over the entire threshold range (0.15–0.26 with an increment of 0.01, involving 12 different thresholds). The regions with values >7 were defined as hubs. Interestingly, the hub regions in the healthy controls were predominantly found in areas of reduced gray matter volume in schizophrenia (Fig. 4). However, regions were differentially sensitive to structural impairments. Specifically, structural impairments in the left precentral gyrus, pars triangularis of left inferior frontal gyrus, and left middle occipital gyrus did not attenuate hub properties, whereas other regions such as medial superior frontal gyrus and bilateral dorsal cingulate gyrus exhibited structural impairments and loss of hub properties (Table 4; supplemental Table S2, available at www.jneurosci.org as supplemental material). Using a $\chi^2$ test, we demonstrated that hub regions were much more likely to have decreased gray matter volume in schizophrenia compared with healthy controls ($p < 0.0001$).

## Discussion

In this study, a number of similarities in functional activations were observed between people with schizophrenia and healthy controls, including regions such as the left lateral frontal, parietal, occipital, insula, and thalamic cortex. These regions have previously been observed to be active in other studies of recollection (Simons and Spiers, 2003; Wagner et al., 2005), as well as those found in source memory studies in healthy subjects (Mitchell and Johnson, 2009). The results from the structural imaging analysis indicated that patients with schizophrenia showed reductions in gray matter volume in the left medial prefrontal cortex, occipital cortex, temporal pole, and bilateral insula, replicating findings in previous studies of brain volume in schizophrenia (Honea et al., 2005). Importantly, there was overlap between functional activations and structural deficits (Table 2) in some of the brain regions. This finding suggests that impaired brain structure did not significantly lead to an altered pattern of functional activation, although it did lead to altered functional connectivity as quantified by small-world properties, emphasizing the importance of combining multimodal approaches.

In this study, similar brain activation patterns across the two groups suggest the same neural networks may be recruited to correctly recall context. However, between-group differences obtained by using liberal statistical threshold ($p < 0.001$, uncorrected) indicated decreased prefrontal activity in schizophrenia, but not a reduction in the medial temporal lobe activity associated with memory processes (Heckers et al., 1998). This negative result with respect to the medial temporal lobe may have been caused by the restriction of the fMRI analysis model to correct recollection trials only, thereby possibly reducing activation differences between groups.

A small-world configuration is a ubiquitous characteristic of complex brain networks and assures functional segregation and integration (Sporns and Zwi, 2004). In general, high global and local efficiency ensure rapid information propagation across distant and neighboring regions, respectively (Latora and Marchiori, 2001). In this study, these network properties were found in

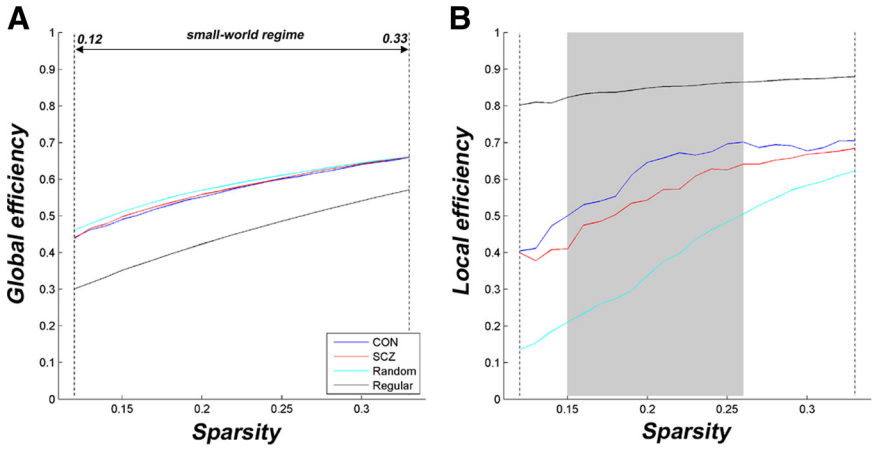


**Figure 3.** Small-world properties of functional brain networks. ***A***, ***B***, The global (***A***) and local (***B***) efficiency are shown as a function of sparsity for random, regular, and real [healthy controls (CON) and schizophrenia patients (SCZ)] networks. For all networks, global and local efficiency increased with the threshold. The global efficiency curves of the real networks are less than those of random networks, but the local efficiency profiles of the real networks are greater than these of the regular networks over the selected threshold range (i.e., between the vertical dash lines), known as a small-world regime. Significant reductions in local efficiency ( $p < 0.05$), but not in the global efficiency, are found in schizophrenia over the threshold range marked by the gray area in ***B***. The random networks were generated by 50 random rewirings of the edges across nodes while keeping the same number of nodes and degree distribution as in the real networks (Sporns and Zwi, 2004). The regular networks were generated by 50 random rewirings of the edges across nodes along the two sides of the main diagonal (Wang et al., 2009).

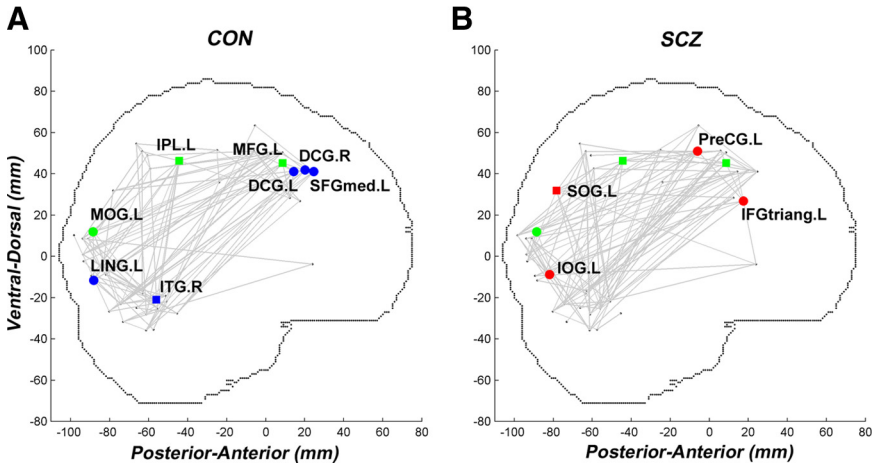


**Figure 4.** Schizophrenia-related changes in network hubs. ***A***, ***B***, The brain networks constructed at the threshold of 0.15 in each group are projected on a sagittal view of the brain in the MNI space for healthy controls (CON; ***A***) and schizophrenia patients (SCZ; ***B***). The small black dots represent the center of each region of 43 activated ROIs. The color-coded regions were identified as network hubs: hubs common to both groups are green, hubs specific to healthy controls are blue, and hubs specific to schizophrenia patients are red. The regions with circles denote structural impairments in schizophrenia. This should be cross-referenced with Table 4. PreCG, precentral gyrus; MFG, middle frontal gyrus; IFGtriang, inferior frontal gyrus (triangular); SFGmed, superior frontal gyrus (medial); DCG, dorsal cingulate gyrus; SOG, superior occipital gyrus; LING, lingual gyrus; MOG, middle occipital gyrus; IPL, inferior parietal lobule; ITG, inferior temporal gyrus; L, left hemisphere; R, right hemisphere.

both healthy controls and patients with schizophrenia (Fig. 3), consistent with a recent study of working memory in schizophrenia (Bassett et al., 2009) and supporting the notion that disease-specific brain networks still possess small-world properties (Bassett and Bullmore, 2009).

Despite this finding, the efficiency profiles of the functional networks were rather different and demonstrated significant group differences in local efficiency. The lack of significant group differences in functional activations excludes the possibility that different activations led to the changes in topographical organization. In contrast, previous studies showing group differences in graph theoretical properties may have been influenced by potential differences in brain activity (Micheloyannis et al., 2006; Liu et al., 2008; Bassett et al., 2009; Rubinov et al., 2009). Altered local efficiency reflects a disturbed balance between local specialization and global integration in schizophrenia. In addition, the power law distribution of degree found in both groups (supplemental Fig. S2, available at www.jneurosci.org as supplemental material) implies that the recollection of contextual memory requires integrated processing over the entire functional network (Gomez Portillo and Gleiser, 2009). Although the observation that schizophrenia patients showed compatible degree distribution with healthy controls assures the ability to efficiently transfer information over task-related regions in schizophrenia patients, it does not prevent decreased local efficiency in the functional network.

In addition, this study identified several important hub regions for contextual memory recollection. They were found predominantly in association regions, which is consistent with prior findings (Achard et al., 2006; Achard and Bullmore, 2007). Our previous studies have demonstrated that hub regions are susceptible to both normal aging and brain disorders (He et al., 2009b; Stam et al., 2009; Wang et al., 2009, 2010a,b). In the current study, some of the hub regions found in healthy controls were located in regions associated with structural deficits in schizophrenia. Moreover, the left middle frontal and inferior parietal cortex were unaffected by structural deficits and were hubs in both groups. Notably, these regions have been hypothesized to play vital roles during recollection (Simons and Spiers, 2003; Wagner et al., 2005). The middle and inferior occipital regions were preserved as hubs in schizophrenia, whereas the medial part of left superior frontal and bilateral anterior cingulate cortex were vulnerable to structural reductions. These results suggest that schizophrenia affects areas important for regional communication and integration. For instance, the dorsal prefrontal regions have been putatively associated with postretrieval monitoring (Achim and Lepage, 2005), which is more critical to the recollection process than the visual processing of the stimulus cues that occurs in the occipital regions. The absence of hubs in key regions in the schizophrenia group, such as dorsal cingulate cortex, suggests that the role of these regions in the networks may be reduced in people with schizophrenia. Previous studies have also demonstrated that schizophrenia patients may experience difficulty monitoring their responses when performing memory retrieval tasks, which has been associated with dorsal cingulate cortex (Vinogradov et al., 2008; Ravizza et al., 2010).

Two limitations of this study should be noted. First, automated voxel-based mophometry methods were used for the anal-

ysis of structural imaging data. This method examines all brain structures simultaneously, which may produce different results than manual tracing techniques. This method of estimating tissue volumes is susceptible to providing misleading results if the sulcal/gyral pattern is abnormal. Studies performed thus far using this technique have not found this, but there is evidence of anomalous cortical gyrification in schizophrenia (Vogeley et al., 2001). Second, many regions that did not show overlap with the functional activations showed reduced gray matter volume as well. It remains unknown whether and how these regions affect functional connectivity patterns of the brain networks. Combining diffusion tensor imaging techniques to track fiber pathways connecting the regions may be required to address this issue.

These results demonstrated that although the same regions form the contextual recollection activation maps in schizophrenia patients and healthy controls, patients showed decreased local network efficiency. Many network hubs found in the schizophrenia group were located in different brain regions than those found in healthy subjects, and this appears to be partly accounted for by lower gray matter volume in schizophrenia. Thus, loss of gray matter volume appears to contribute to differences in the architecture of the network in schizophrenia. The findings suggest that the core pathophysiological problem underlying contextual memory impairments in schizophrenia might be disruptive alterations in the coordination of large-scale brain networks, and this may be affected by structural deficits.

## References


Achard S, Bullmore E (2007) Efficiency and cost of economical brain functional networks. PLoS Comput Biol 3:e17.

Achard S, Salvador R, Whitcher B, Suckling J, Bullmore ET (2006) A resilient, low-frequency, small-world human brain functional network with highly connected association cortical hubs. J Neurosci 26:63–72.

Achim AM, Lepage M (2005) Neural correlates of memory for items and for associations: an event-related functional magnetic resonance imaging study. J Cogn Neurosci 17:652–667.

Ammons RB, Ammons CH (1962) The Quick Test (QT). Missoula, MT: Psychological Test Specialists.

Balota DA, Yap MJ, Cortese MJ, Hutchison KA, Kessler B, Loftis B, Neely JH, Nelson DL, Simpson GB, Treiman R (2007) The English Lexicon Project. Behav Res Methods 39:445–459.

Bassett DS, Bullmore ET (2009) Human brain networks in health and disease. Curr Opin Neurol 22:340–347.

Bassett DS, Bullmore ET, Meyer-Lindenberg A, Apud JA, Weinberger DR, Coppola R (2009) Cognitive fitness of cost-efficient brain functional networks. Proc Natl Acad Sci U S A 106:11747–11752.

Bezchlibnyk-Butler KZ, Jeffries JJ (2005) Clinical handbook of psychotropic drugs, Ed 15. Seattle: Hogrefre and Huber.

Bressler SL, Kelso JA (2001) Cortical coordination dynamics and cognition. Trends Cognit Sci 5:26–36.

Bullmore E, Sporns O (2009) Complex brain networks: graph theoretical analysis of structural and functional systems. Nat Rev Neurosci 10:186–198.

Cairo TA, Liddle PF, Woodward TS, Ngan ETC (2004) The influence of working memory load on phase specific patterns of cortical activity. Cognit Brain Res 21:377–387.

Eguiluz VM, Chialvo DR, Cecchi GA, Baliki M, Apkarian AV (2005) Scale-free brain functional networks. Phys Rev Lett 94:018102.

Friston KJ, Frith CD, Liddle PF, Frackowiak RS (1993) Functional connectivity: the principal-component analysis of large (PET) data sets. J Cereb Blood Flow Metab 13:5–14.

Gomez Portillo IJ, Gleiser PM (2009) An adaptive complex network model for brain functional networks. PLoS One 4:e6863.

Gur RC, Gur RE (1995) Hypofrontality in schizophrenia: RIP. Lancet 345:1383–1384.

Hayasaka S, Phan KL, Liberzon I, Worsley KJ, Nichols TE (2004) Nonstationary cluster-size inference with random field and permutation methods. Neuroimage 22:676–687.

He Y, Chen Z, Gong G, Evans A (2009a) Neuronal networks in Alzheimer's disease. Neuroscientist 15:333–350.

He Y, Dagher A, Chen Z, Charil A, Zijdenbos A, Worsley K, Evans A (2009b) Impaired small-world efficiency in structural cortical networks in multiple sclerosis associated with white matter lesion load. Brain 132:3366–3379.

Heckers S, Rauch SL, Goff D, Savage CR, Schacter DL, Fischman AJ, Alpert NM (1998) Impaired recruitment of the hippocampus during conscious recollection in schizophrenia. Nat Neurosci 1:318–323.

Heinrichs RW, Zakzanis KK (1998) Neurocognitive deficit in schizophrenia: a quantitative review of the evidence. Neuropsychology 12:426–445.

Hollingshead AB, Redlich FC (1958) Social class and mental illness. New York: Wiley.

Honea R, Crow TJ, Passingham D, Mackay CE (2005) Regional deficits in brain volume in schizophrenia: a meta-analysis of voxel-based morphometry studies. Am J Psychiatry 162:2233–2245.

Honey CJ, Sporns O, Cammoun L, Gigandet X, Thiran JP, Meuli R, Hagmann P (2009) Predicting human resting-state functional connectivity from structural connectivity. Proc Natl Acad Sci U S A 106:2035–2040.

Kiss GR, Armstrong C, Milroy R, Piper J (1973) An associative thesaurus of English and its computer analysis. In: The computer and literary studies (Aitkin AJ, Bailey RW, Hamilton-Smith N, eds), pp 153–165. Edinburgh: University Press.

Latora V, Marchiori M (2001) Efficient behavior of small-world networks. Phys Rev Lett 87:198701.

Liddle PF, Ngan ET, Duffield G, Kho K, Warren AJ (2002) Signs and Symptoms of Psychotic Illness (SSPI): a rating scale. Br J Psychiatry 180:45–50.

Liu Y, Liang M, Zhou Y, He Y, Hao Y, Song M, Yu C, Liu H, Liu Z, Jiang T (2008) Disrupted small-world networks in schizophrenia. Brain 131:945–961.

Lund K, Burgess C (1996) Producing high-dimensional semantic spaces from lexical co-occurrence. Behav Res Methods Instrum Comput 28:203–208.

MacDonald AW 3rd, Carter CS, Kerns JG, Ursu S, Barch DM, Holmes AJ, Stenger VA, Cohen JD (2005) Specificity of prefrontal dysfunction and context processing deficits to schizophrenia in never-medicated patients with first-episode psychosis. Am J Psychiatry 162:475–484.

Micheloyannis S, Pachou E, Stam CJ, Breakspear M, Bitsios P, Vourkas M, Erimaki S, Zervakis M (2006) Small-world networks and disturbed functional connectivity in schizophrenia. Schizophr Res 87:60–66.

Mitchell KJ, Johnson MK (2009) Source monitoring 15 years later: what have we learned from fMRI about the neural mechanisms of source memory? Psychol Bull 135:638–677.

Ravizza SM, Moua KC, Long D, Carter CS (2010) The impact of context processing deficits on task-switching performance in schizophrenia. Schizophr Res 116:274–279.

Rissman J, Gazzaley A, D'Esposito M (2004) Measuring functional connectivity during distinct stages of a cognitive task. Neuroimage 23:752–763.

Rubinov M, Knock SA, Stam CJ, Micheloyannis S, Harris AW, Williams LM, Breakspear M (2009) Small-world properties of nonlinear brain activity in schizophrenia. Hum Brain Mapp 30:403–416.

Ruff CC, Woodward TS, Laurens KR, Liddle PF (2001) The role of the anterior cingulate cortex in conflict processing: evidence from reverse Stroop interference. Neuroimage 14:1150–1158.

Rushworth MF, Hadland KA, Paus T, Sipila PK (2002) Role of the human medial frontal cortex in task switching: a combined fMRI and TMS study. J Neurophysiol 87:2577–2592.

Sheehan DV, Lecrubier Y, Sheehan KH, Amorim P, Janavs J, Weiller E, Hergueta T, Baker R, Dunbar GC (1998) The Mini-International Neuropsychiatric Interview (M.I.N.I.): the development and validation of a structured diagnostic psychiatric interview for DSM-IV and ICD-10. J Clin Psychiatry 59[Suppl 20]:22–33; quiz 34–57.

Simons JS, Spiers HJ (2003) Prefrontal and medial temporal lobe interactions in long-term memory. Nat Rev Neurosci 4:637–648.

Simons JS, Davis SW, Gilbert SJ, Frith CD, Burgess PW (2006) Discriminating imagined from perceived information engages brain areas implicated in schizophrenia. Neuroimage 32:696–703.

Sporns O, Zwi JD (2004) The small world of the cerebral cortex. Neuroinformatics 2:145–162.

Stam CJ, de Haan W, Daffertshofer A, Jones BF, Manshanden I, van Cappellen van Walsum AM, Montez T, Verbunt JP, de Munck JC, van Dijk BW, Berendse HW, Scheltens P (2009) Graph theoretical analysis of magnetoencephalographic functional connectivity in Alzheimer's disease. Brain 132:213–224.

Strogatz SH (2001) Exploring complex networks. Nature 410:268–276.

Tzourio-Mazoyer N, Landeau B, Papathanassiou D, Crivello F, Etard O, Delcroix N, Mazoyer B, Joliot M (2002) Automated anatomical labeling of activations in SPM using a macroscopic anatomical parcellation of the MNI MRI single-subject brain. Neuroimage 15:273–289.

van den Heuvel MP, Stam CJ, Boersma M, Hulshoff Pol HE (2008) Small-world and scale-free organization of voxel-based resting-state functional connectivity in the human brain. Neuroimage 43:528–539.

Vinogradov S, Luks TL, Schulman BJ, Simpson GV (2008) Deficit in a neural correlate of reality monitoring in schizophrenia patients. Cereb Cortex 18:2532–2539.

Vogeley K, Tepest R, Pfeiffer U, Schneider-Axmann T, Maier W, Honer WG, Falkai P (2001) Right frontal hypergyria differentiation in affected and unaffected siblings from families multiply affected with schizophrenia: a morphometric mri study. Am J Psychiatry 158:494–496.

Wagner AD, Shannon BJ, Kahn I, Buckner RL (2005) Parietal lobe contributions to episodic memory retrieval. Trends Cogn Sci 9:445–453.

Wang L, Zhu C, He Y, Zang Y, Cao Q, Zhang H, Zhong Q, Wang Y (2009) Altered small-world brain functional networks in children with attention-deficit/hyperactivity disorder. Hum Brain Mapp 30:638–649.

Wang L, Li Y, Metzak P, He Y, Woodward TS (2010a) Age-related changes in topological patterns of large-scale brain functional networks during memory encoding and recognition. Neuroimage 50:862–872.

Wang L, Yu C, Chen H, Qin W, He Y, Fan F, Zhang Y, Wang M, Li K, Zang Y, Woodward TS, Zhu C (2010b) Dynamic functional reorganization of the motor execution network after stroke. Brain 133:1224–1238.

Watts DJ, Strogatz SH (1998) Collective dynamics of "small-world" networks. Nature 393:440–442.

Woodward TS, Ruff CC, Ngan ET (2006a) Short- and long-term changes in anterior cingulate activation during resolution of task-set competition. Brain Res 1068:161–169.

Woodward TS, Meier B, Cairo TA, Ngan ET (2006b) Temporo-prefrontal coordination increases when semantic associations are strongly encoded. Neuropsychologia 44:2308–2314.